



AIAA 94-0597 ASTER Instrument Design and Science Objectives

Y. Yamaguchi and H. Tsu
Geological Survey of Japan
Tsukuba, Japan

H. Fujisada
Electrotechnical Laboratory
Tsukuba, Japan

A. Kahle and D. Nichols
Jet Propulsion Laboratory, California Institute of
Technology
Pasadena, CA

**32nd Aerospace Sciences
Meeting & Exhibit**
January 10-13, 1994 / Reno, NV

ASTER INSTRUMENT DESIGN AND SCIENCE OBJECTIVES

Y. Yamaguchi and H. Tsu
Geological Survey of Japan
1-1-3 Higashi, Tsukuba
Ibaraki, 305 Japan

H. Fujisada
Electrotechnical Laboratory
1-1-4 Urnezono, Tsukuba
Ibaraki, 305 Japan

A. Kahle and D. Nichols
Jet Propulsion Laboratory
California Institute of Technology
4800 Oak Grove Drive
Pasadena, CA 91109

Abstract

The Advanced Spaceborne Thermal Emission and Reflection Radiometer (ASTER), a multi-spectral imaging radiometer with 14 spectral bands, is a research facility instrument that will be launched in 1998 on NASA's EOS AM-1 platform. Characteristics of the ASTER data can be summarized as (1) wide spectral coverage from the visible to thermal infrared regions, (2) multispectral thermal infrared data with high spectral and spatial resolution and (3) along-track stereoscopic capability. ASTER is currently being designed and fabricated to meet the requirements given by the ASTER Science Team,

1. Introduction

Advanced Spaceborne Thermal Emission and Reflection Radiometer (ASTER) is a research facility instrument proposed by the Ministry of International Trade and Industry (MITI) of Japan to be launched on NASA's EOS AM-1 platform in 1998. The primary science objective of the ASTER mission is to improve understanding of the local- and regional-scale processes occurring on or near the Earth's surface and lower atmosphere, including surface-atmosphere interactions.

Specific areas of the science investigation can be listed as: (a) geology and soil - the detailed compositional and geomorphologic mapping of surface soil and bedrock to study the land surface processes and the Earth's history; (b) vegetation and ecosystem dynamics - investigations of vegetation and soil distribution and their changes to estimate biological productivity to understand land-atmosphere interaction and to detect ecosystem changes; (c) land surface climatology - investigation of land surface parameters, surface temperature etc., to understand land-atmosphere interaction and energy and moisture fluxes; (d) volcano monitoring - monitoring of eruptions and precursive events such as emission of volcanic gases to the atmosphere, eruption plumes, development of lava lakes and fumarolic activity, eruptive history and eruptive potential; (e) aerosols and clouds - observation of atmospheric aerosol characteristics and various cloud types, which are useful for the atmospheric correction of surface retrievals; (f) evapotranspiration - the knowledge of the difference between air temperature measured in situ and canopy temperature derived from ASTER radiance measurements; (g) carbon cycling and marine ecosystem - the atmospheric carbon dioxide being fixed into coral reefs by measuring the global distribution and accumulation rate of coral reefs; and (h) hydrology - understanding global energy and hydrologic processes and their relationship to global changes.

Copyright © 1994 by the American Institute of Aeronautics and Astronautics. All rights reserved.

Subsystem	Band	Spectral Range (μm)	Radiometric Resolution	Spatial Resolution
VNIR	1	0.52-0.60	$\leq 0.5\%$	15 m
	2	0.63-0.69		
	3	0.76-0.86		
	4	1.60-1.70		
SWIR	5	2.145-2.185	$\leq 1.3\%$	30 m
	6	2.185-2.225	$\leq 1.3\%$	
	7	2.235-2.285	$\leq 1.3\%$	
	8	2.295-2.365	$\leq 1.0\%$	
	9	2.36-2.43	$\leq 1.3\%$	
	10	8.125-8.475		
TIR	11	8.475-8.825	$\leq 0.3\text{ K}$	90 m
	12	8.925-9.275		
	13	10.25-10.95		
	14	10.95-11.65		
Stereo B/H Ratio			0.6	
Swath Width			60 km	
Pointing Capability in the Cross-track Direction			$\pm 116\text{ km}$	

Table 1 ASTER baseline performance requirements.

Table 1 shows the baseline performance requirements for ASTER. The optical signal sensing units of the instrument consists of three subsystems as shown in Figure 1; the visible and near-infrared (VNIR) radiometer, short-wave-infrared (SWIR) radiometer, and thermal infrared (TIR) radiometer. ASTER has three spectral bands in the VNIR, six bands in the SWIR, and five bands in the TIR regions with 15, 30, and 90 m ground resolution respectively. All bands will cover the same 60 km ground swath. A pointing capability in the cross-track direction will allow coverage of $\pm 116\text{ km}$ from the nadir. The VNIR subsystem has one backward-viewing band for stereo-mpic observation in the along-track direction. Because the data will have wide spectral coverage and relatively high spatial resolution, we will be able to discriminate a variety of surface materials and reduce problems resulting from mixed pixels. ASTER will provide the highest spatial resolution surface temperature and emissivity data of all the EOS AM-1 instruments.

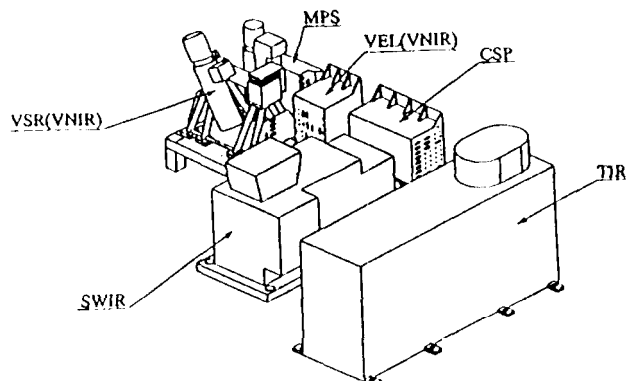


Figure 1 ASTER on-orbit configuration.

2. Design Status

Figure 2 shows the functional block diagram of the ASTER instrument. The VNIR, SWIR, and TIR subsystems receive optical signals from the ground, convert them into electrical signals and send the signals to a common signal processor (CSP) as digital data. The CSP multiplexes signals from the three subsystems with system telemetry, and sends them to the platform electronics in the proper format. The master power supply (MPS) provides electric power to each ASTER component by converting the power provided from the spacecraft.

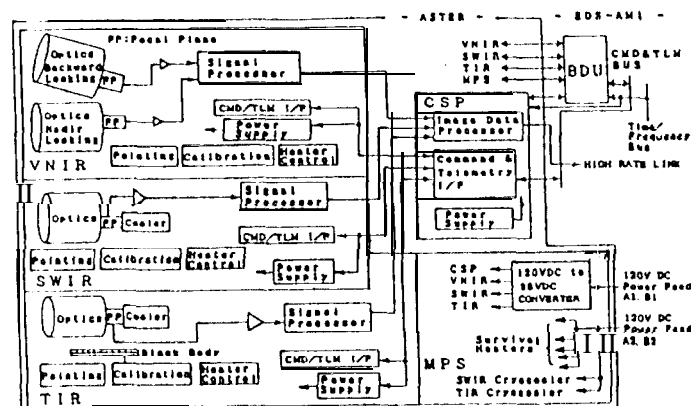


Figure 2 Block diagram of the ASTER instrument.

Table 2 summarizes the characteristics of the ASTER subsystems. The three optical subsystems consist of collection optics, spectral separation units, focal plane assemblies, calibration modules, control units, power supply unit and signal processing electronics respectively. In addition, the SWIR and TIR subsystems have mechanical coolers to cool the detectors, and the TIR subsystem has a scanning mirror,

Subsystem	Scan	Telescope Optics	Spectral Separation	Focal plane (Detectors)	Cooler	Crosstrack Pointing
VNIR	Pushbroom	Re flect (Schmidt) D=82.25mm (W=94.28mm (H)	Dichroic bandpass & filters	Si-CCD S000 X 1	not cooled	Telescope inclination ($\pm 24^\circ$)
SWIR	Pushbroom	Refractive D=190mm	Bandpass filters	PtSi-CCD 2100 X 8	Stirling cycle (80 K)	Pointing mirror ($\pm 0.55^\circ$)
TIR	Whiskbroom	Reflective (Newtonian) D=240mm	Bandpass filters	HgCdTe (PC) 10 X 5	Stirling cycle (80 K)	Scan mirror ($\pm 0.55^\circ$)

Table 2 Characteristics of the ASTER subsystems.

Different telescope types are employed for the three subsystems in order to optimize the optics in the different wavelength regions; Schmidt-type reflective optics for the VNIR, refractive optics for the SWIR, and Newtonian-type reflective optics for the TIR. Spectral separation in all bands will be made by bandpass filters.

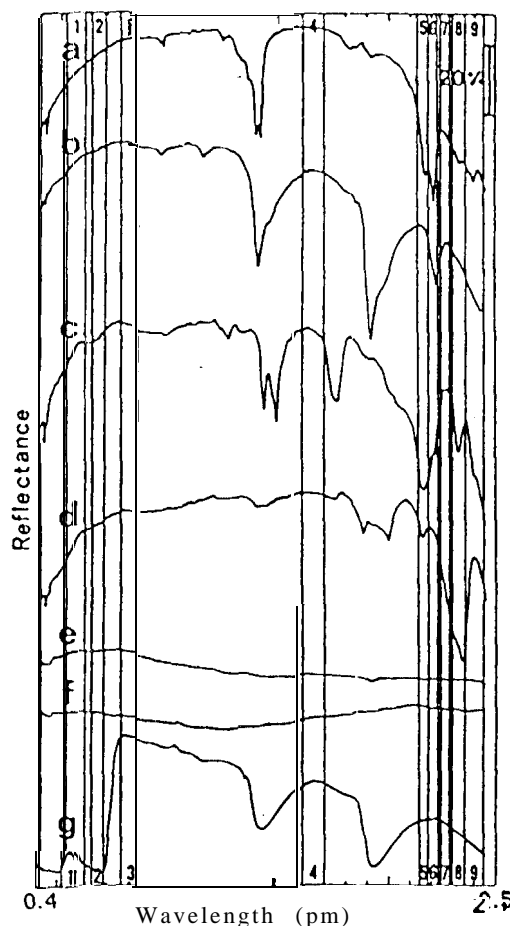


Figure 3a Spectral bandpasses of the ASTER VNIR and SWIR, and the reflectance spectra of typical minerals, rocks and Vegetation: (a) kaolinite; (b) montmorillonite; (c) alunite; (d) calcite; (e) andesite; (f) granite; (g) green leaves.

VNIR and SWIR images are obtained by pushbroom scanning with linear array detectors. Each spectral band of the VNIR has a linear Si-CCD detector with 5000 elements. The SWIR subsystem has a linear PtSi-CCD detector with 2100 elements for each spectral band. The TIR subsystem uses mechanical scanning with 10 HgCdTe PC-type detectors for each spectral band, thus there are 50

total TIR detectors. The SWIR and TIR subsystems have long life Stirling-cycle cryocoolers to cool the detectors to 80 K or below. The design life is 50,000 hours on-orbit, which corresponds to the 5 year mission period of the EOS AM-I spacecraft.

3. Performance Requirements

Spectral performance

The ASTER has 14 spectral bands. The three VNIR bands have the similar bandpasses to those of the Landsat Thematic Mapper (TM) and the Optical Sensor (OPS) of the Japanese Earth Resources Satellite (JERS-1), as shown in Figure 3a. The VNIR bands will be used for topographic interpretation because of the 15 m spatial resolution. The VNIR bands will also be useful in assessing vegetation and iron oxide minerals in surface soils and rocks

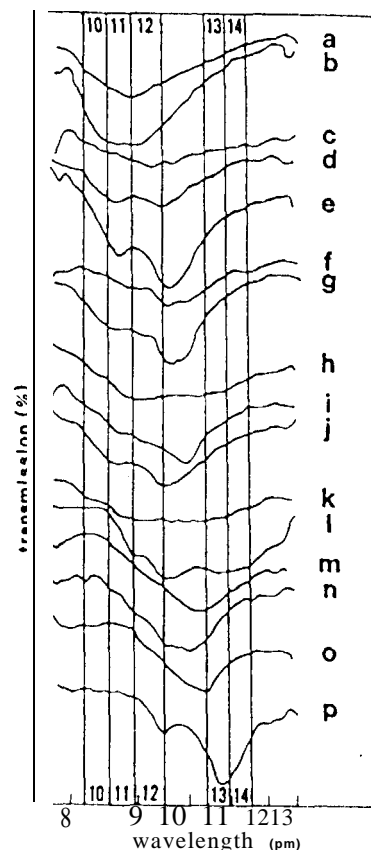


Figure 3b Spectral bandpasses of the ASTER TIR, and the emissivity (transmission) spectra of typical rocks (modified from Vickers and Lyon, 1967): (a) dacite; (b) granite; (c) pumice; (d) trachyte; (e) quartz syenite; (f) andesite; (g) nephelene syenite; (h) hypersthene andesite; (i) quartz diorite; (j) augite diorite; (k) basalt; (l) plagioclase basalt; (m) peridotite; (n) serpentinite; (o) limburgite; (p) dunite.

The spectral bandpasses of the SWIR bands were selected mainly for the purpose of surface mineralogical mapping. Band 4 is centered at the 1.65 micron region, and bands 5 to 9 target the characteristic absorption features of phyllosilicate and carbonate minerals in the 2.1 to 2.4 micron region. The ASTER SWIR will permit more detailed surface lithologic mapping than Landsat TM and JERS-1 OPS. Discrimination of clouds from snow will also be possible using the SWIR bands.

The ASTER TIR subsystem has 5 bands in the thermal infrared region as shown in Figure 3b. Emissivity patterns derived from the five TIR bands will be used to estimate silica content, which is important in characterizing silicate rocks -- the most abundant rock type on the earth's surface. The ASTER Science Team is developing algorithms to separate temperature and emissivity of surface targets.

Radiometric Performance

The user requirements for radiometric performance were given as noise-equivalent-reflectance (NE $\Delta\rho$) for the VNIR and SWIR subsystems as shown in Table 1. However, since the instrument parameter defining the radiometric resolution is signal-to-noise ratio (SNR), the NE $\Delta\rho$ is translated into SNR by using the relation; SNR = (target reflectance / NE $\Delta\rho$). For the TIR bands, the radiometric resolution is specified directly by user requirements for noise-equivalent- temperature (NE ΔT), which is also convenient for instrument performance tests. The requirement is applied to the high level input radiance, which is shown in Table 3, unless otherwise specified. The signal quantization level is specified as 8 bits for the VNIR and SWIR subsystems, and 12 bits for the TIR subsystem.

Subsystem	Band No.	Maximum Input Radiance	High Level Input Radiance	Low Level Input Radiance
VNIR	1	427	356	71.2
	2	358	298	59.6
	3N	218	182	36.4
	3B	218	182	36.4
SWIR	4	55.0	45.8	9.16
	5	17.6	14.7	2.94
	6	15.8	13.2	2.64
	7	15.1	12.6	2.52
TIR	8	10.55	8.79	1.78
	9	04	6.70	1.34
	10~14	Radiance of 370K Blackbody	Radiance of 300K Blackbody	Radiance of 200 K Blackbody

Table 3 Input radiances [W/(m²sr μ m)] for the ASTER spectral bands.

User requirements for the absolute radiometric accuracy of the VNIR and SWIR bands are ± 4 percent or less at the high level input radiance. The absolute radiometric accuracy for the TIR bands is defined as ± 3 K or less in

the range from 200-240 K, ± 2 K or less in the range from 240-270 K, ± 1 K or less in the range from 270-340 K, and ± 2 K in the range from 340-370 K.

Subsystem	Band No.	High Gain	Normal Gain	Low Gain-1	Low Gain-2
VNIR	1	2.5	1.0	0.75	N/A
	2	2.0	1.0	0.75	N/A
	3	2.0	1.0	0.75	N/A
	4	2.0	1.0	0.75	0.75 (TBR)
SWIR	5	2.0	1.0	0.75	0.17 (TBR)
	6	2.0	1.0	0.75	0.16 (TBR)
	7	2.0	1.0	0.75	0.18 (TBR)
	8	2.0	1.0	0.75	0.17 (TBR)
TIR	9	2.0	1.0	0.75	0.12 (TBR)
	10~14	N/A	1.0	N/A	N/A

Table 4 Gain switching function (multiplication factors).

The VNIR and SWIR subsystems have three and four gain settings respectively as shown in Table 4. The gain setting for each band can be selected independently. The high gain setting is used to expand a range of output DN's for a low reflectance target. The low gain setting is provided to accommodate an unexpectedly bright target, although almost all targets are expected to be observable by the normal gain. The low gain-2, available only for the SWIR bands, will be used for observation of high temperature targets such as a lava lake of an active volcano. Table 5 shows the highest temperatures observable by the SWIR bands, as calculated from the saturation levels of the CCD detector array.

Band No.	Low Gain-2 Multipl. Factor	Saturation Input Radiance (W/m ² sr μ m)	Corresponding Temperature (K)
4	0.75	73.3	739
5	0.17	103.5	658
6	0.16	98.7	649
7	0.18	83	631
8	0.17	62.0	603
9	0.12	67.0	599

Table 5 SWIR saturation levels and the highest observable temperature.

Geometric Performance

Spatial resolution of the ASTER subsystems is 15 m for VNIR, 30 m for SWIR, and 90 m for TIR. The VNIR has the highest spatial resolution, along with a stereo imaging capability, so the VNIR data will be quite useful for topographic interpretation. The spatial resolution of the SWIR and TIR are lower than the VNIR, but are still the highest among all the EOS AM-1 instruments in their wavelength regions. ASTER data are expected to provide important information for sub-pixel scale analysis of data from other EOS AM-1 instruments, e.g., MODIS and MISR.

Band-to-band registration (BBR) requirements from the ASTER Science Team are ± 0.2 pixels in the same telescope and ± 0.3 pixels (of the coarser spatial resolution) among the different telescopes, after ground processing. The ability to meet these requirements is determined in part by the ability to accurately position the detectors in the fabrication process. The detector configuration accuracy is specified as shown in Table 6. The bias is a fixed deviation from an ideal detector configuration which would exhibit no misregistration. For the VNIR and SWIR subsystems, resampling is necessary for precise BBR, even within the same telescope. Stability is specified so as to maintain the BBR of 0.2 pixels or less during the mission period, because we would like to assure the BBR accuracy within each telescope with an accuracy of ± 0.2 pixels by using only the preflight parameters of the focal plane configuration. Since the TIR subsystem employs mechanical scanning, the BBR specification within the telescope will be possible without resampling.

Subsystem	Bias		Stability (3 σ)
	Along-track	Cross-track	
VNIR	± 3 pixels	± 6 pixels	± 0.2 pixels
SWIR	± 410 pixels	± 0.2 pixels	± 0.2 pixels
TIR	± 0.05 pixels	± 0.05 pixels	N/A

Table 6 Specification of the detector configuration accuracy.

For the BBR among the different telescopes, correlation processing will be carried out to find a set of geometric coefficients for every orbit or every eight minutes of data acquisition. If the instrument is kept at the same pointing position, the same geometric coefficients can be used over an 8 minute data segment due to an expected stability of ± 0.1 pixels.

Stereo Capability

The nadir-backward stereo viewing geometry of the VNIR results in a higher probability of obtaining a cloud-free image pair, as compared with a side-nadir stereo observation system such as the SPOT HRV. Taking into account the earth rotation effect, the linear detector arm ys of the backward-viewing bands have about 5000 detector elements that allow 60 km overlap in a stereo pair within the range of 60 degrees north and south latitude.

The base-height (BH) ratio of 0.6, which roughly corresponds to a vertical exaggeration factor of 4 in visual stereoscopic observation, is an appropriate value for photogeologic interpretation in mountain terrain. The

stereo images will also be used for studies on three-dimensional cloud structures.

Digital elevation models (DEM) can be generated from stereo data. The height accuracy of the DEM depends upon the BH ratio, spatial resolution, and error in the parallax measurement. The ASTER DEM height precision would be 12.5 or 25 m, and the scale of topographic maps to be generated from the ASTER stereo data would be 1:1 00,000 to 1:200,000 respectively, if we assume 0.5 to 1.0 pixel as the total parallax error. The ability to control the parallax error depends on the availability and accuracy of ground control points.

Pointing Capability

All ASTER bands will cover the same 60 km imaging swath with a pointing capability in the cross-track direction to cover ± 116 km from the nadir, so that any point on the globe is accessible at least once every 16 days with the full spectral coverage with the VNIR, SWIR and TIR.

In addition, the VNIR subsystem has a larger pointing capability, up to 24 degrees, and thus the swath center is pointable up to ± 318 km from the nadir. This capability was added in order to shorten the potential delay period for a time-critical observation of natural hazards like volcanic eruptions and floods. The recurrent pattern for a target on the equator using the 24 degrees pointing becomes 2-4-2-7 days (4 days average).

Operations Modes

The ASTER instrument consists of three subsystems which can be operated independently. Combined with multiple gain settings and pointing angles, there are many possible combinations of observation modes, however, several nominal modes have been defined. The nominal daytime mode is simultaneous data acquisition using the three subsystems looking at the same 60 km imaging swath. The nominal nighttime mode is TIR-only operation. Flexibility in operations has been requested from the ASTER Science Team in order to obtain as much data as possible while keeping within the allocated data rate. Therefore, three additional nominal modes have been recognized such that all nominal modes are defined as;

- 1) Daytime full mode (VNIR + SWIR + TIR)
- 2) Daytime VNIR mode (VNIR)
- 3) Daytime DEM mode (VNIR bands 3N and 3B)
- 4) Nighttime TIR mode (TIR)
- 5) Nighttime volcano monitoring mode (TIR + SWIR)

One Orbit Average Maximum Observation Time				Two Orbit Average Maximum Observation Time					
Type	Combination		Number of Observation	Total observation Time (minutes)	Type	Combination		Number of Observation	Total Observation Time (minutes)
C1	Day	V/S/T 1)	Continuous	16	C2	Day	V/S/T 1)	Continuous	8
	1-	V•Stereo 2)	Continuous	0,94		1-	V•Stereo 2)	Continuous	0.94
	Night	T	Continuous	4		Night	T	Continuous	2
D13)	Day	V/S/T 1)	5	16	D23)	Day	V/S/T 1)	3	8
	Day	V•Stereo 2)	1	4.70		Day	V•Stereo 2)	3	2.82
	Night	T	1	2		Night	T	1	2

1) The full mode operation, V/S/T, includes stereo band observation.

2) The operation of V•Stereo is for the overhead time and follows the full mode operation.

3) The period between observations is assumed to be 3 minutes.

Table 7 Examples of operations scenarios.

The daytime VNIR mode will be used for areas where high resolution VNIR data are essential, but SWIR and TIR spectral data are not necessary. If a pointing angle of greater than 8.55 is needed, the daytime VNIR or DEM mode has to be used, since the SWIR and TIR can only be pointed up to 8.55 degrees. In the daytime DEM mode, only the bands 3N (nadir) and 3B (backward) will be operated for the purpose of stereo imaging. These two modes are complementary to the daytime full mode, and will be used only when allocated resources cannot permit the full mode. For instance, periodic monitoring of the Antarctic glacier boundaries, using the VNIR data is one objective of the ASTER Science Team which can be satisfied by the daytime DEM mode.

During nighttime, the TIR mode is the nominal operational mode. However, it will be possible to use the SWIR bands at night. Such an occasion might arise if a target temperature is higher than the maximum input radiance for the TIR bands (i.e. a radiance of 370 K blackbody in front of the radiometer), which could occur with a high temperature target like a lava lake or flow of an active volcano.

The ASTER instrument duty cycle is limited by data rate, electric power consumption, thermal design, and on-off cycling. The maximum data rate is defined by a two orbit average value. The maximum average data rate allocated to ASTER is 8.3 Mbps, which roughly corresponds to 8 minutes of full-mode daytime operation plus 8 minutes of nighttime TIR operation. The single orbit maximum data acquisition time is 16 minutes. The

maximum number of discrete continuous observation segments per orbit is currently 15, 5, and 6 for VNIR, SWIR and TIR respectively. The ASTER Science Team is investigating alternative operations strategies taking these constraints into account. Table 7 shows examples of constraints associated with the instrument operations modes.

Data Products

Table 8 shows a list of data products proposed by the ASTER Science Team. The Japanese are responsible for providing ASTER Level-1 data products. For the standard data products, all algorithms produced in both Japan and U.S. will be identical, although the source code and executable programs may be different. Algorithm development is being carried out collaboratively by Japan and the U.S. Standard data products will be provided to users from the U.S. EOSDIS and the Japanese ASTER

	Japan	U.S.
Reconstructed, unprocessed instrument data	○	○
Radiance, registered at sensor	○	○
Relative spectral emissivity	○	○
Relative spectral reflectance	○	○
Surface radiance	○	○
Surface temperature	○	○
Surface emissivity	○	○
Surface reflectance	○	○
Cartographically appeal	○	○
Scene classification	○	○
Digital elevation model	○	○
Brightness temperature at sensor	○	○
Normalized difference vegetation index	○	○
Vegetation & soil indices	○	○
Polar cloud map	○	○

Table 8 ASTER standard data products.

5. Summary

The preliminary design review (PDR) of the ASTER instruments was completed in February, 1993. According to the PDR results, the ASTER instrument will meet the user **requirements** which are **described** in this paper, and will be delivered to NASA on **schedule**. The ASTER **Science Team** is now developing algorithms to generate data **products** using the information provided from the ASTER Instrument Team.

6. Acknowledgements

The instrument development activities described in this **paper are** being carried out by the Japanese Ministry of International Trade and Industry (MITI). The associated **science activities described** herein are being carried out partially by MITI; and partially by the Jet Propulsion Laboratory, California Institute of Technology, under a **contract** with the National Aeronautics and Space Administration.

7. References

1. Y. Yamaguchi, H. Tsu and H. Fujisada, Scientific *Basis of ASTER Instrument Design*, SPIE Proc. v.1939, p.150-160, 1993.
2. H. Fujisada and A. One, *Anticipated Performance of ASTER Instrument in EM Design Phase*, SPIE Proc. v.1939, p.187-197, 1993.
3. R. S. Vickers and R. J. P. Lyon, *Infrared Sensing from Spacecraft - A Geologic Interpretation*, Proc. Thermophysics Spec. Conf., American Institute of Astronautics, Paper 67-284, 1967.